Electronic Supplementary Material (ESI) for New Journal of Chemistry.
This journal is © The Royal Society of Chemistry and the Centre National de la Recherche Scientifique 2018

Gold Doping Induced Strong Enhancement of Carbon Quantum Dots Fluorescence and Oxygen Evolution Reaction Catalytic Activity of Amorphous Cobalt Hydroxide

Pandi Muthukumar and Savarimuthu Philip Anthony*

Department of Chemistry, School of Chemical & Biotechnology, SASTRA University, Thanjavur-613401, Tamil Nadu, India. E-mail: philip@biotech.sastra.edu.

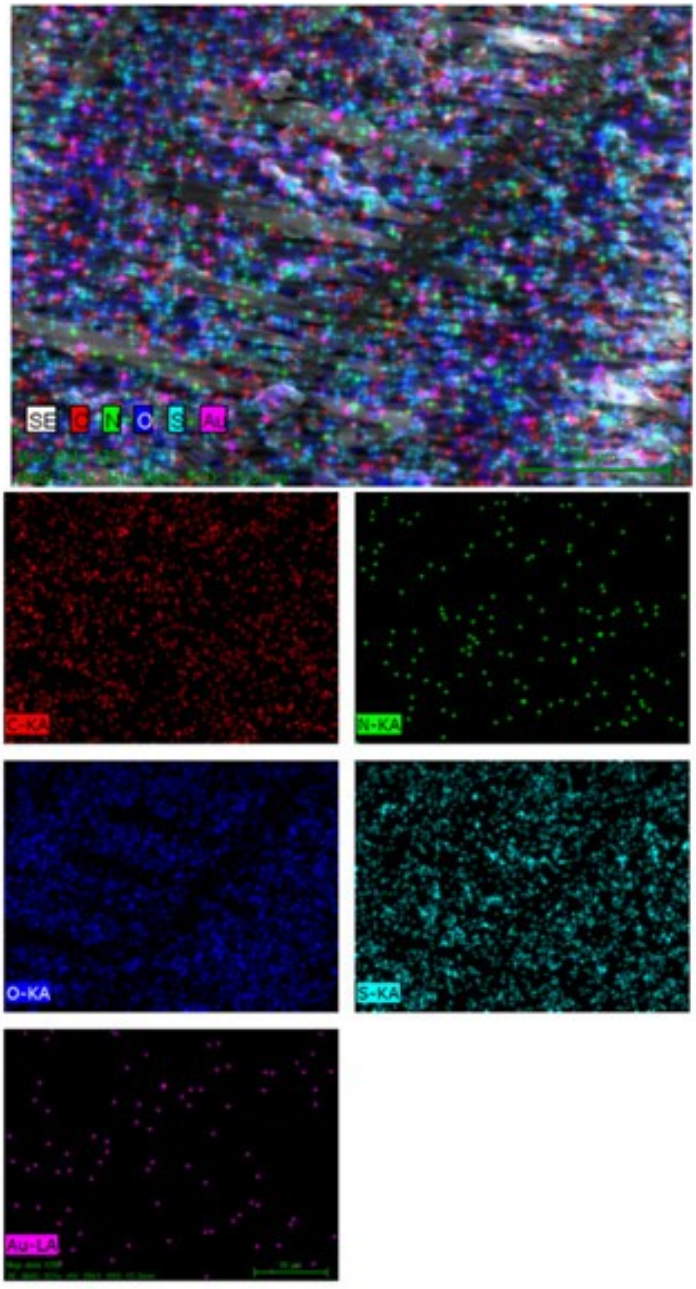

Figure S1. Elemental mapping analysis of Au-SCQDs-10.

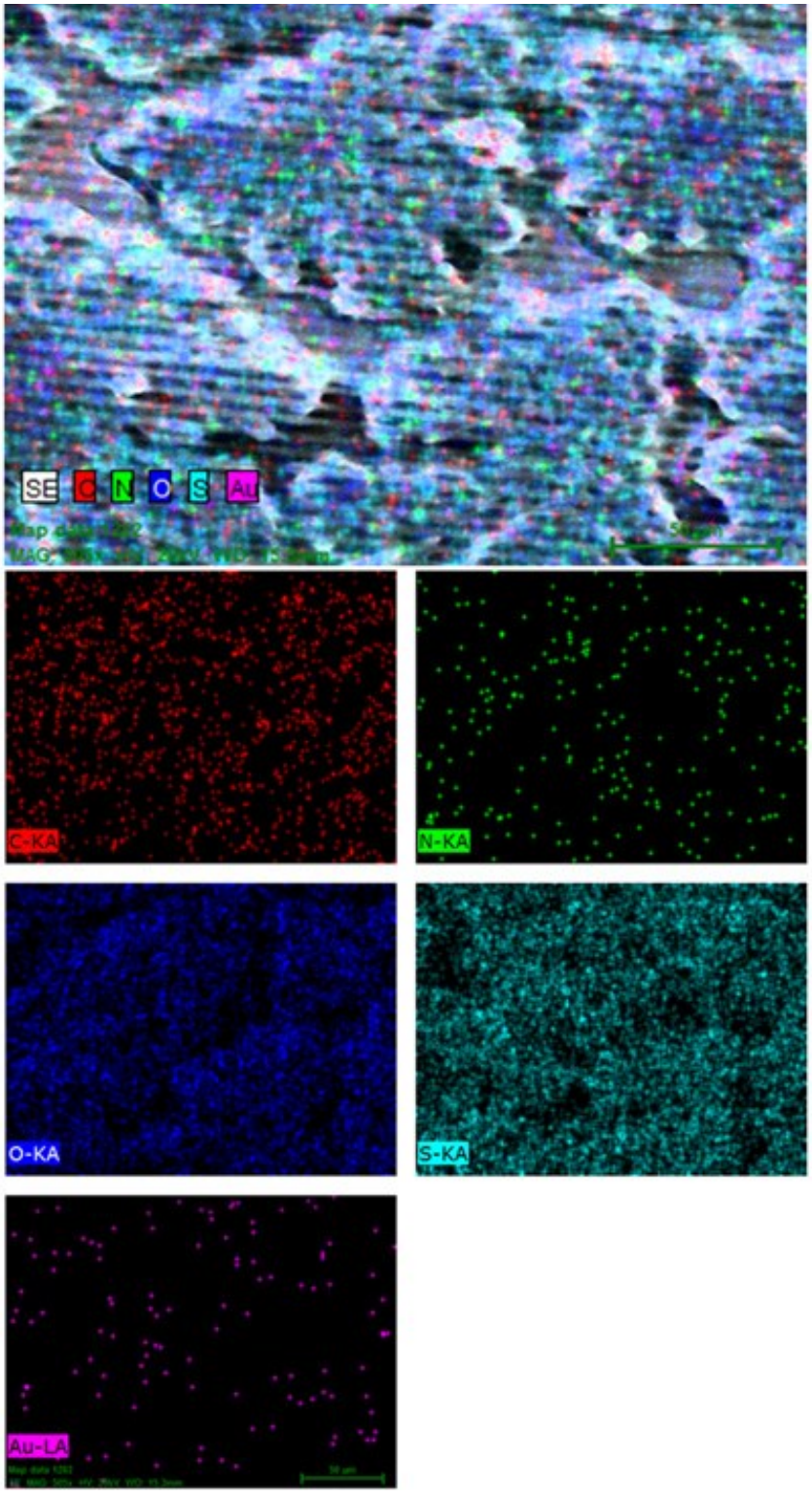

Figure S2. Elemental mapping analysis of Au-SCQDs- 40.

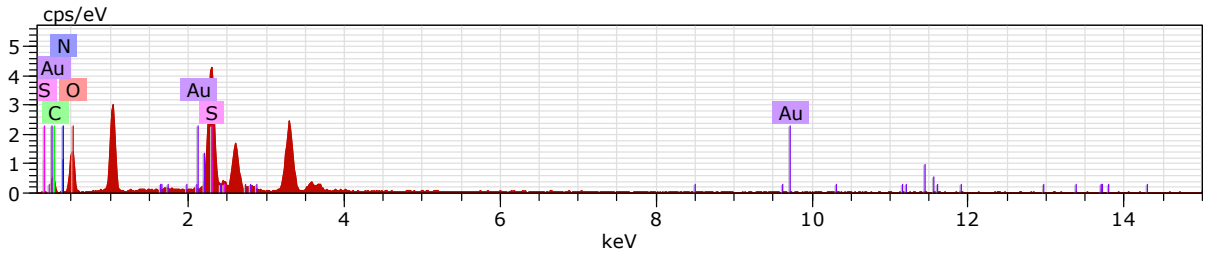

sample 20922 Date:03-Mar-18 3:35:10 PM HV:30.0kV Puls th.:2.41kcps

El	AN	Series	unn. C [wt.%]	norm. C [wt.%]	Atom. C [at.%]	Error (1 Sigma) [wt.%]
O	8	K-series	29.71	52.91	51.22	6.38
C	6	K-series	17.48	31.12	40.13	5.29
S	16	K-series	7.98	14.21	6.86	0.35
N	7	K-series	0.90	1.60	1.77	1.10
Au	79	L-series	0.09	0.16	0.01	0.05

Fig. S3. EDX analysis of Au-SCQDs-10.

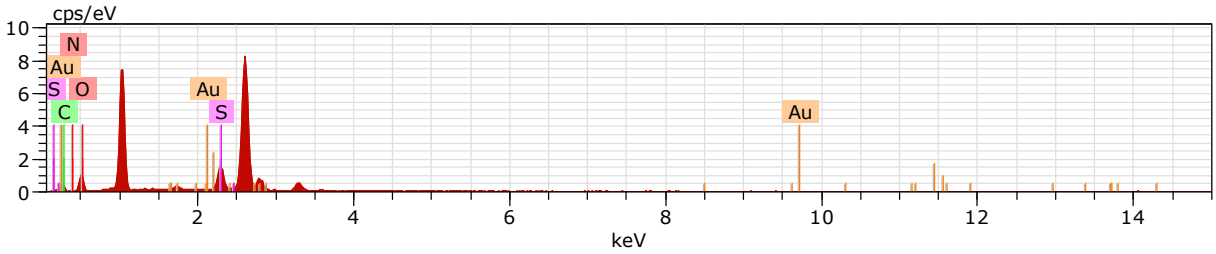

sample 20936 Date:03-Mar-18 3:52:12 PM HV:30.0kV Puls th.:2.67kcps

El	AN	Series	unn. C [wt.%]	norm. C [wt.%]	Atom. C [at.%]	Error (1 Sigma) [wt.%]
O	8	K-series	55.40	55.40	51.51	12.45
C	6	K-series	34.29	34.29	42.47	9.88
S	16	K-series	7.64	7.64	3.54	0.38
N	7	K-series	2.31	2.31	2.45	2.59
Au	79	L-series	0.37	0.37	0.03	0.12

Fig. S4. EDX analysis of Au-SCQDs-20.

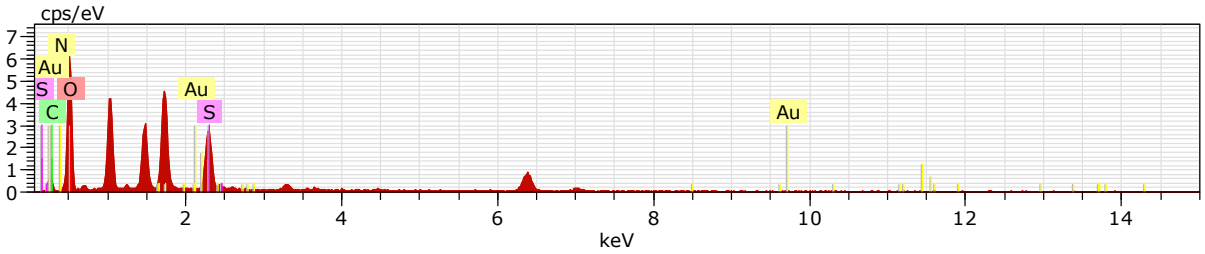

sample 20929 Date:03-Mar-18 3:43:36 PM HV:30.0kV Puls th.:2.95kcps

El	AN	Series	unn. C [wt.%]	norm. C [wt.%]	Atom. C [at.%]	Error (1 Sigma) [wt.%]
O	8	K-series	74.82	74.82	72.55	11.75
C	6	K-series	16.93	16.93	21.87	4.68
N	7	K-series	2.66	2.66	2.94	1.63
S	16	K-series	5.42	5.42	2.62	0.26
Au	79	L-series	0.18	0.18	0.01	0.07

Fig. S5. EDX analysis of Au-SCQDs-40.

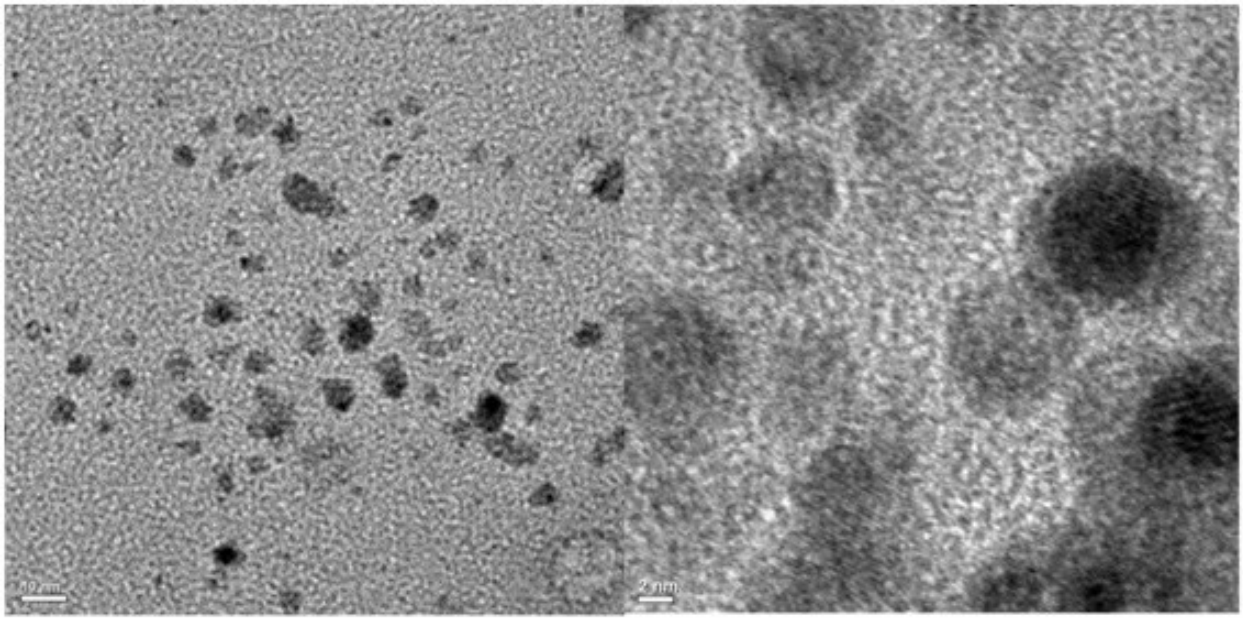

Figure S6. HR-TEM images of SCQDs.

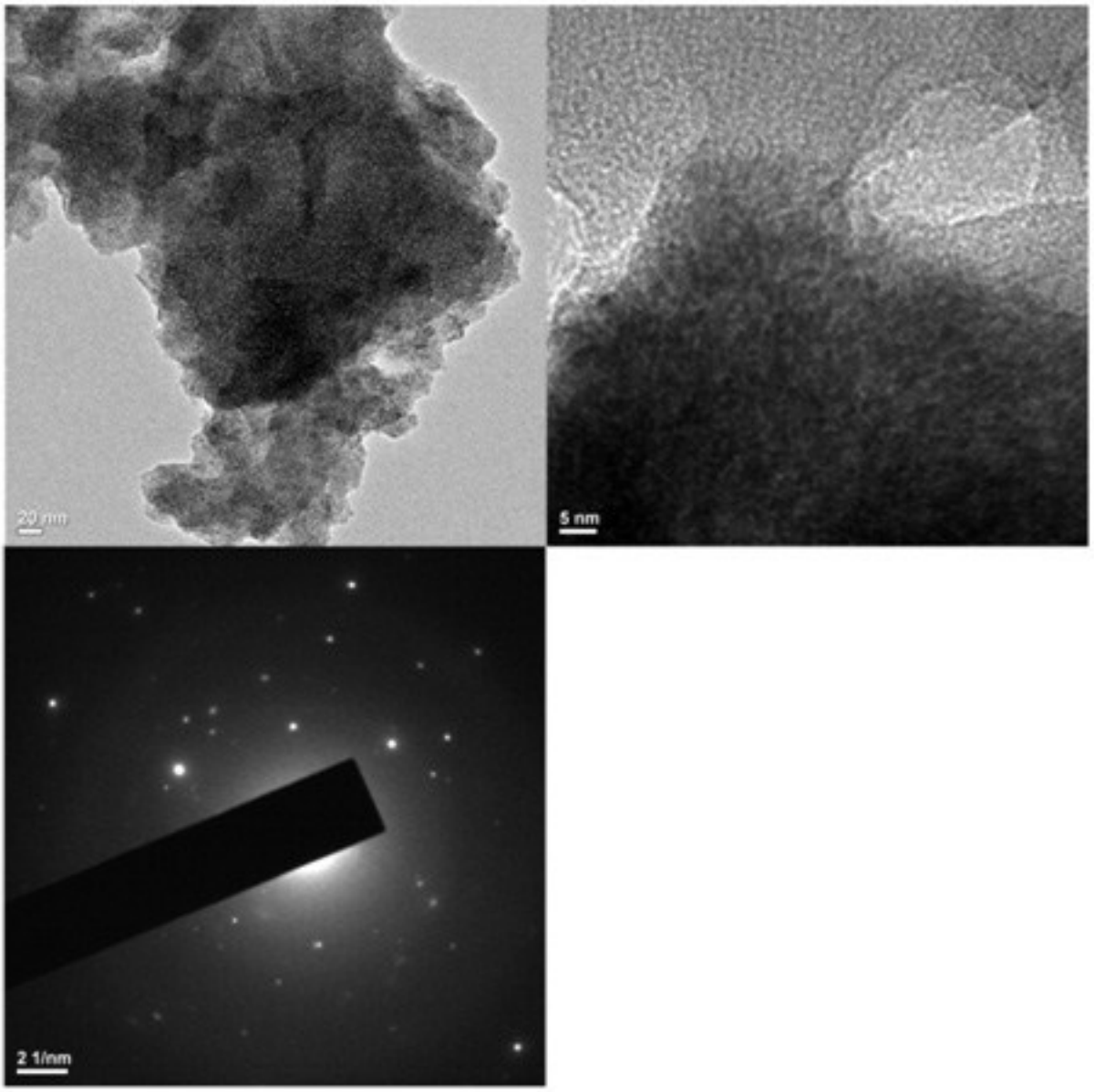

Figure S7. HR-TEM images of Au-SCQDs-10.

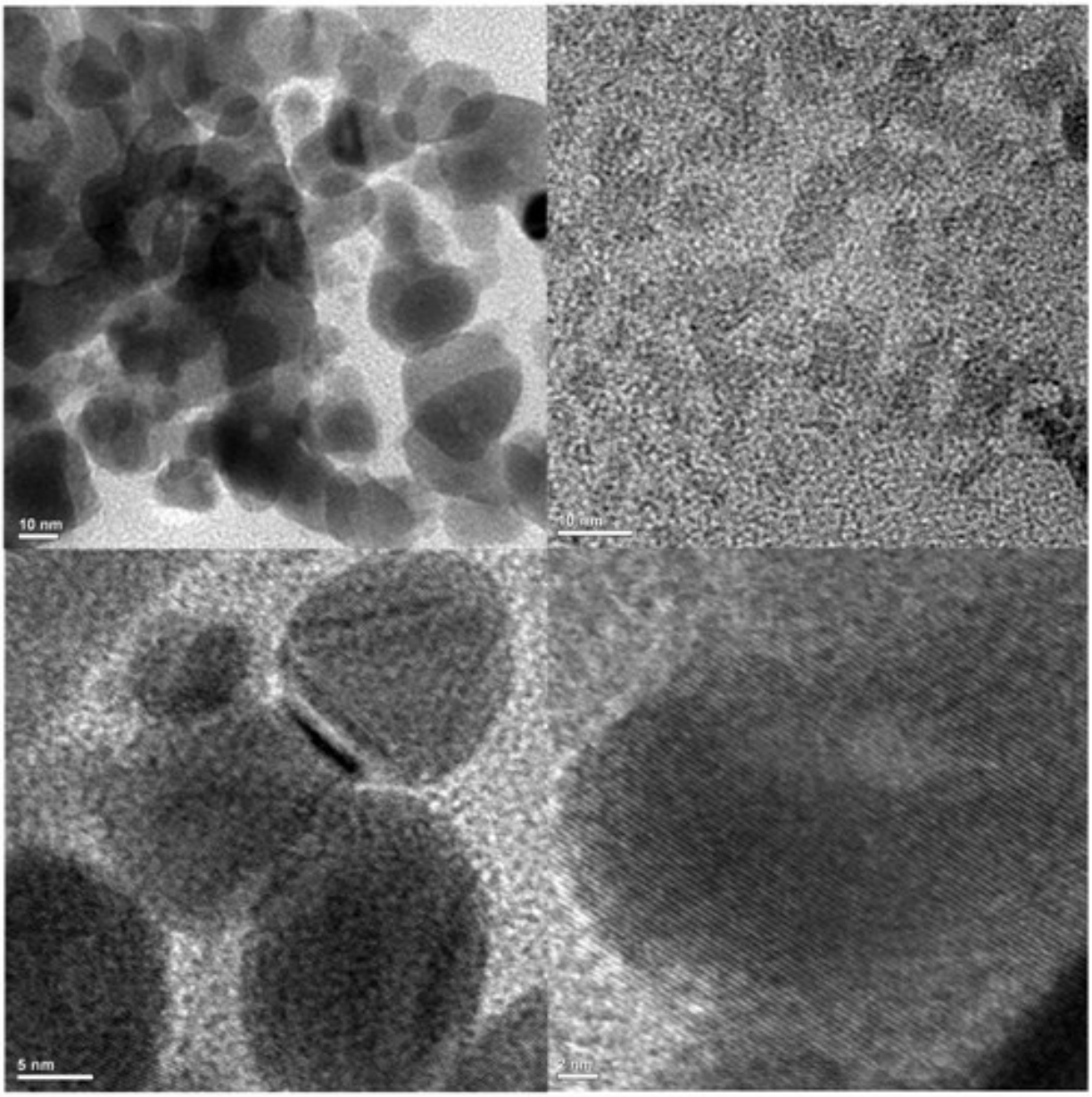

Figure S8. HR-TEM images of Au-SCQDs-20.

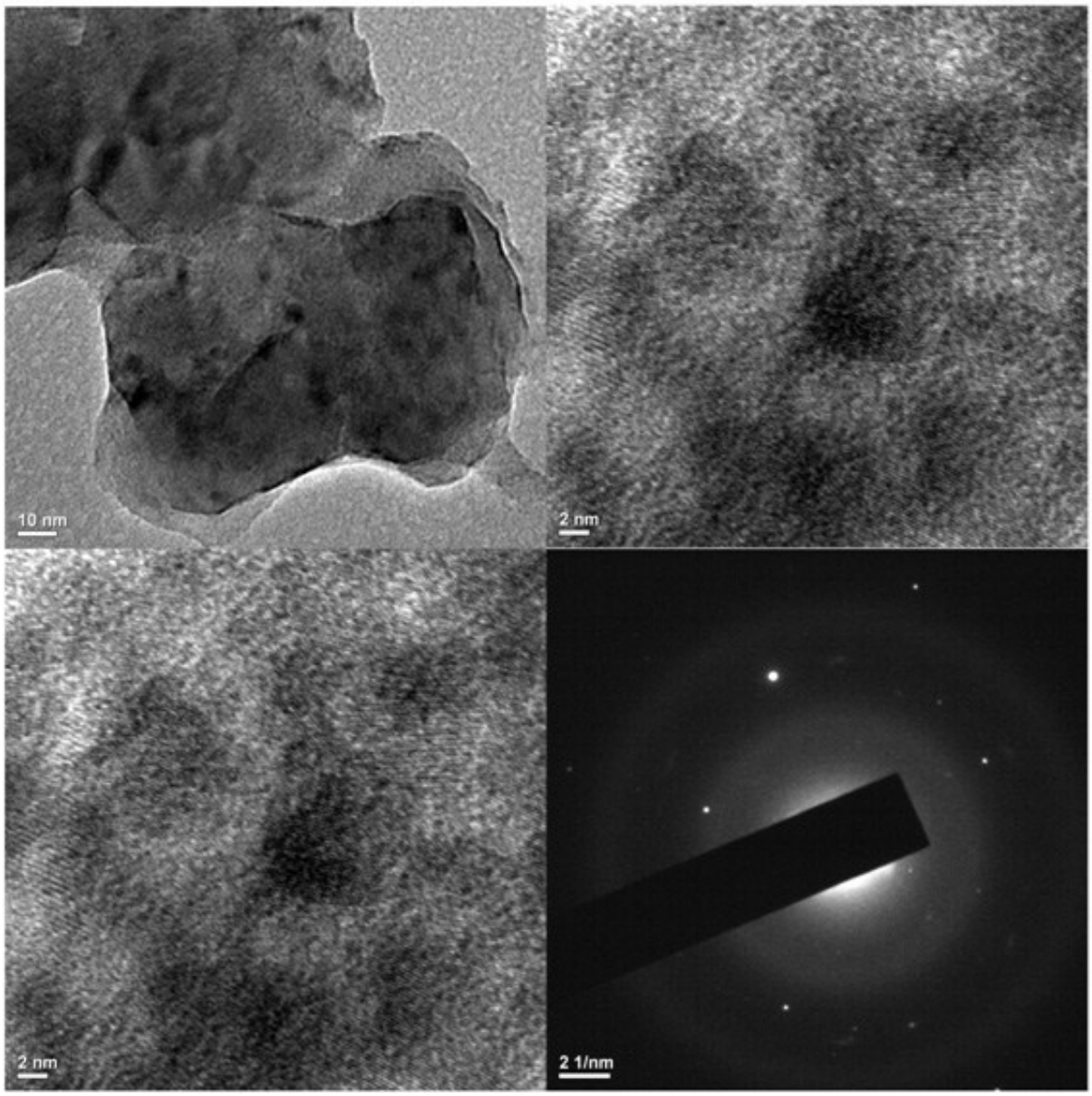

Figure S9. HR-TEM images of Au-SCQDs-40.

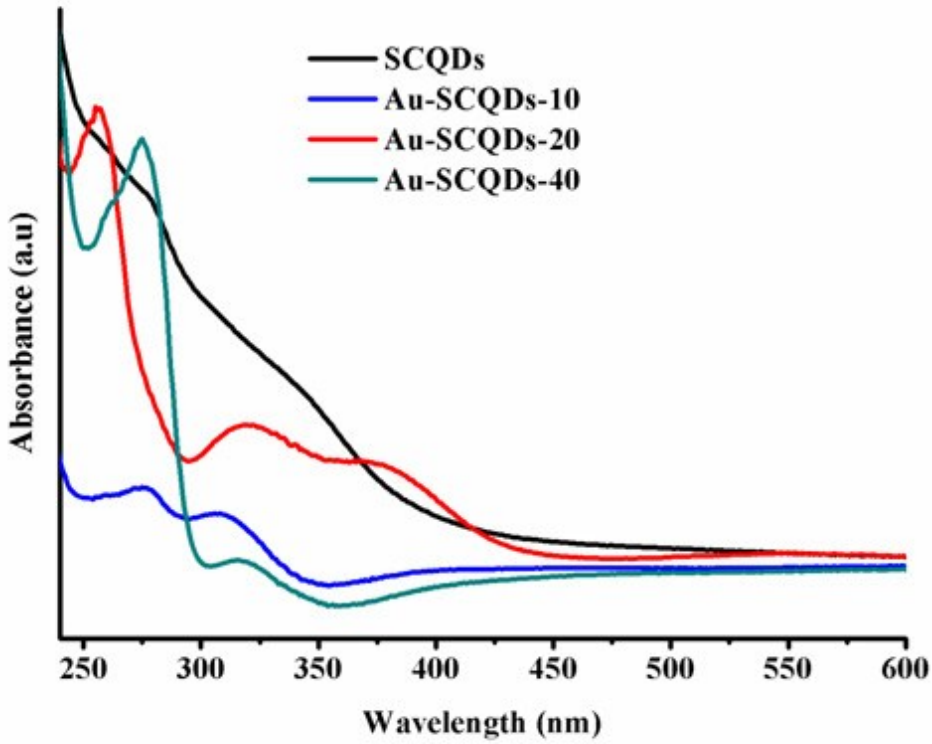

Figure S10. Absorption spectra of Au-SCQDs-10, 20 and 40.

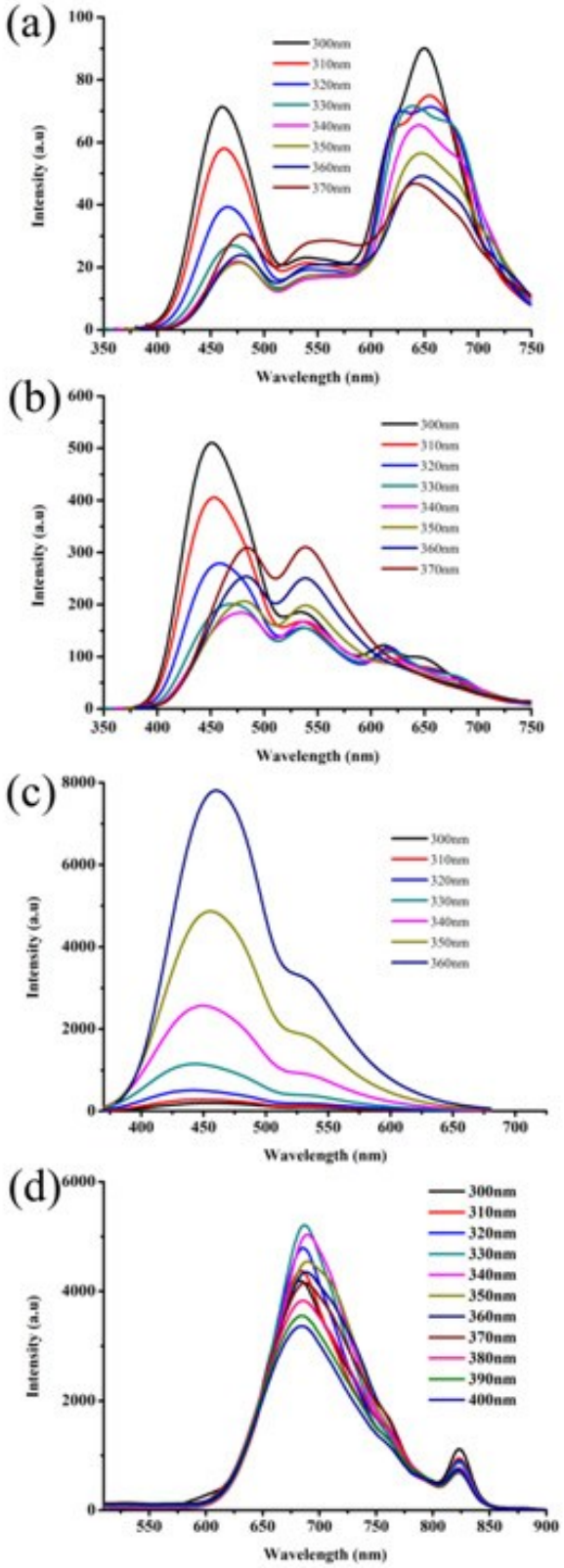

Figure S11. Fluorescence spectra of (a) SCQDs, (b) Au-SCQDs-10, (c) Au-SCQDs-20 and(d) Au-SCQDs -40 at different excitation wavelength.

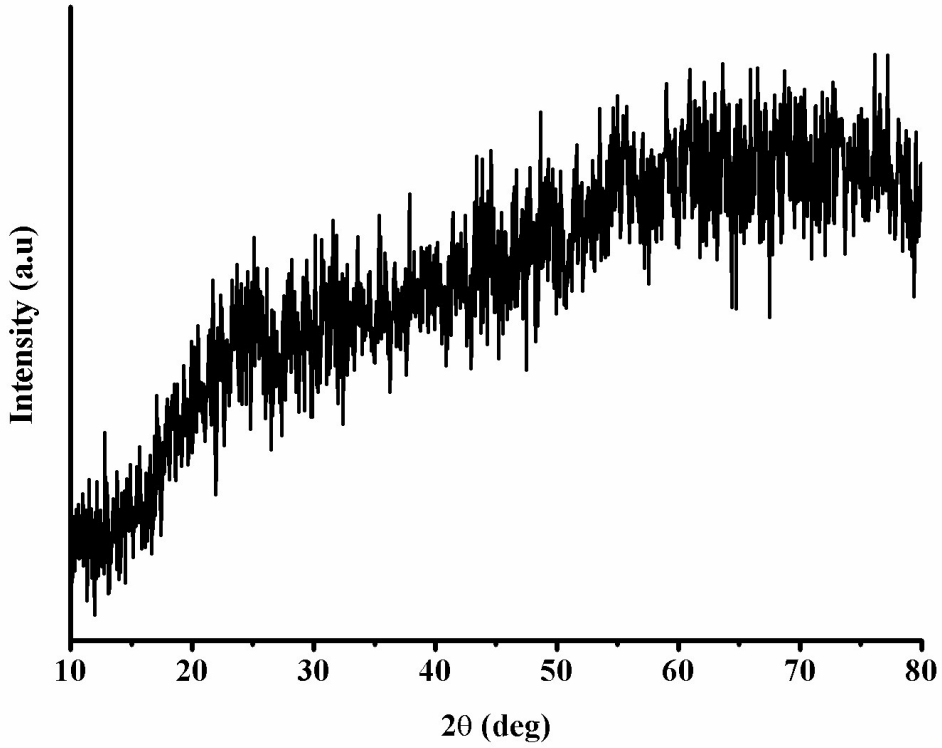

Figure S12. PXRD pattern of $Co(OH)_2$-Au-SCQDs-20

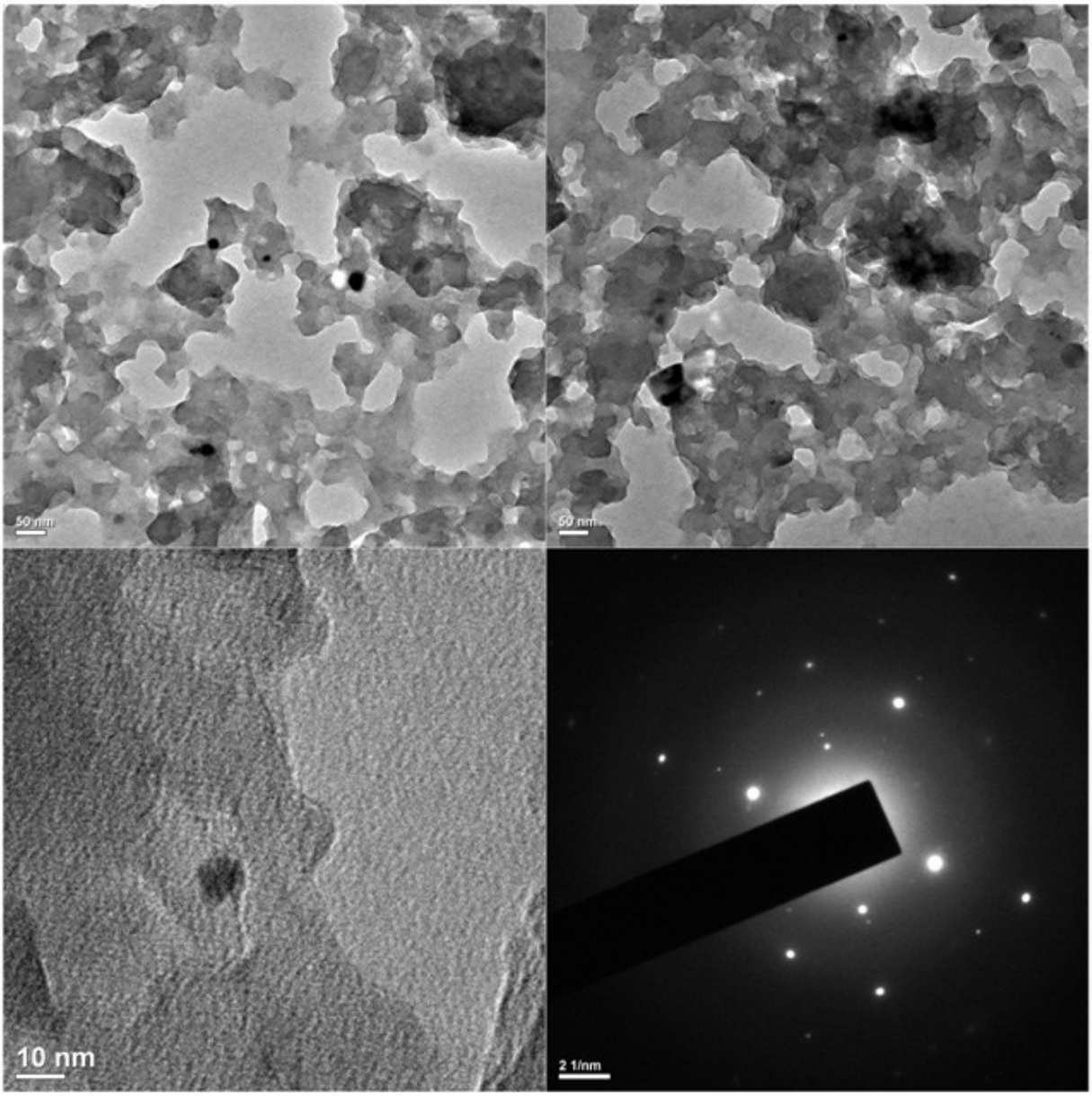

Figure S13. HR-TEM images of (a, b) $Co(OH)_2$-Au-SCQDs-10 (c) fringe pattern and (d) selected area diffraction pattern.

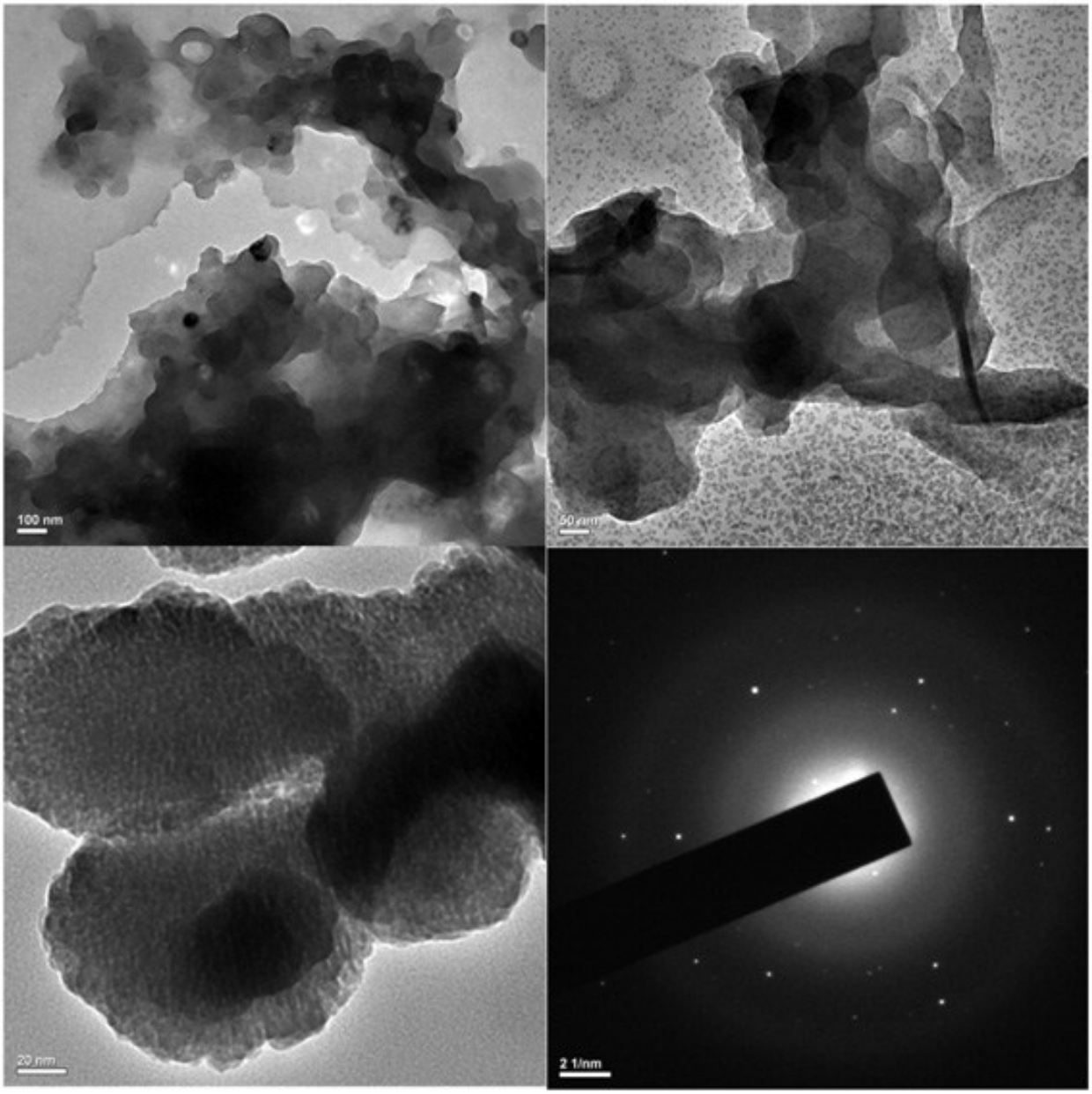

Figure S14. HR-TEM images of (a, b) $Co(OH)_2$-Au-SCQDs-40 (c) fringe pattern and (d) selected area diffraction pattern.

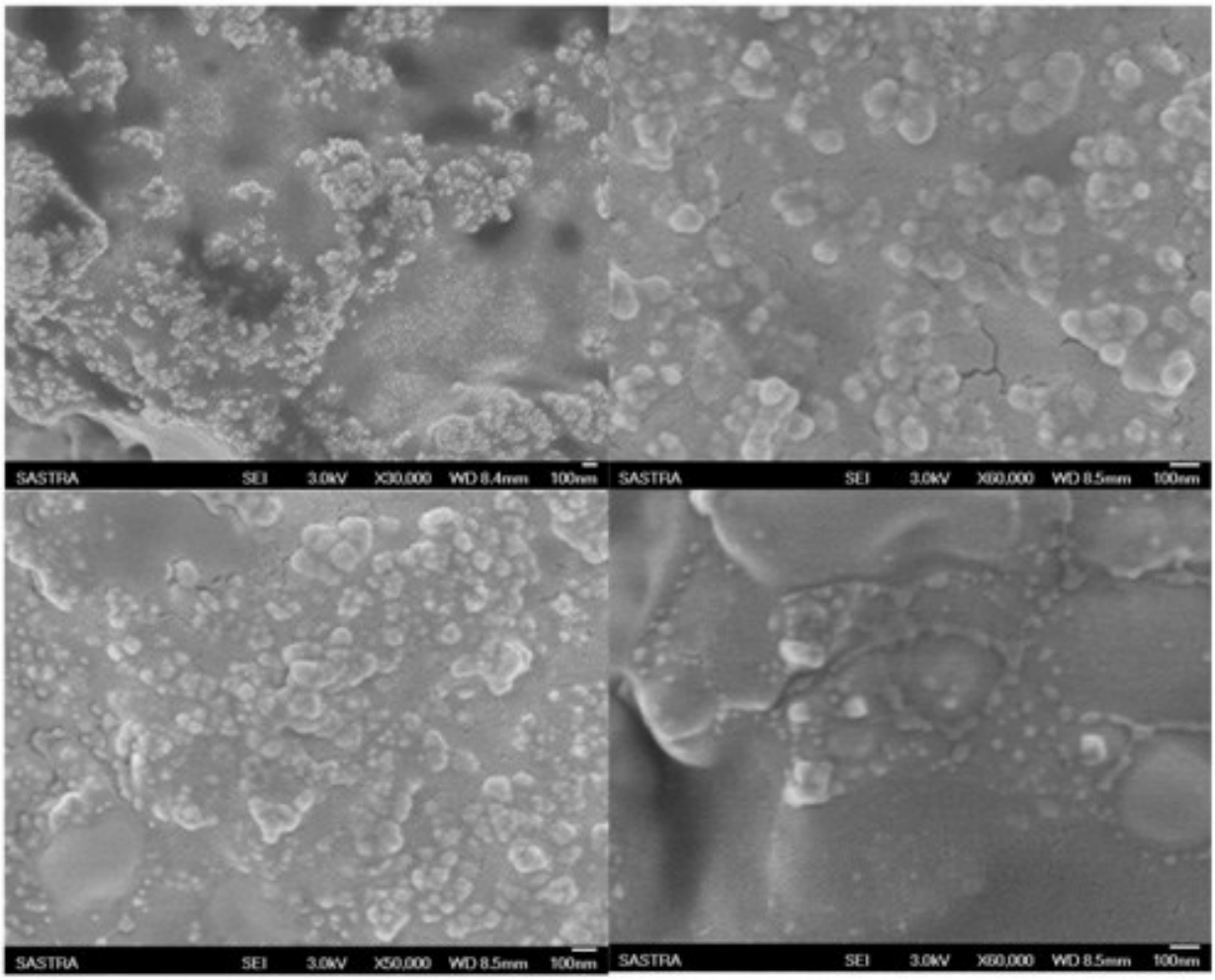

Figure S15. FE-SEM images of $Co(OH)_2$-Au-SCQDs-20.

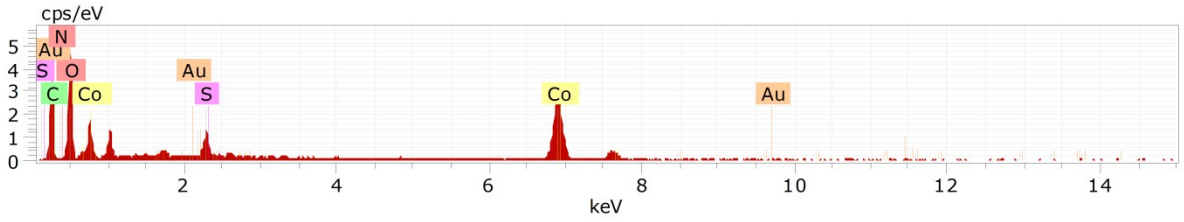

sample 20933 Date:03-Mar-18 3:47:35 PM HV:30.0kV Puls th.:2.64kcps

El	AN	Series	unn. C [wt.%]	norm. C [wt.%]	Atom. C [at.%]	Error (1 Sigma) [wt.%]
O	8	K-series	82.27	48.86	47.19	13.07
C	6	K-series	60.51	35.94	46.23	10.40
N	7	K-series	4.77	2.83	3.13	2.42
Co	27	K-series	18.82	11.18	2.93	0.55
S	16	K-series	1.77	1.05	0.51	0.11
Au	79	L-series	0.22	0.13	0.01	0.07

Figure S16. Elemental mapping of $Co(OH)_2$-Au-SCQDs-20.

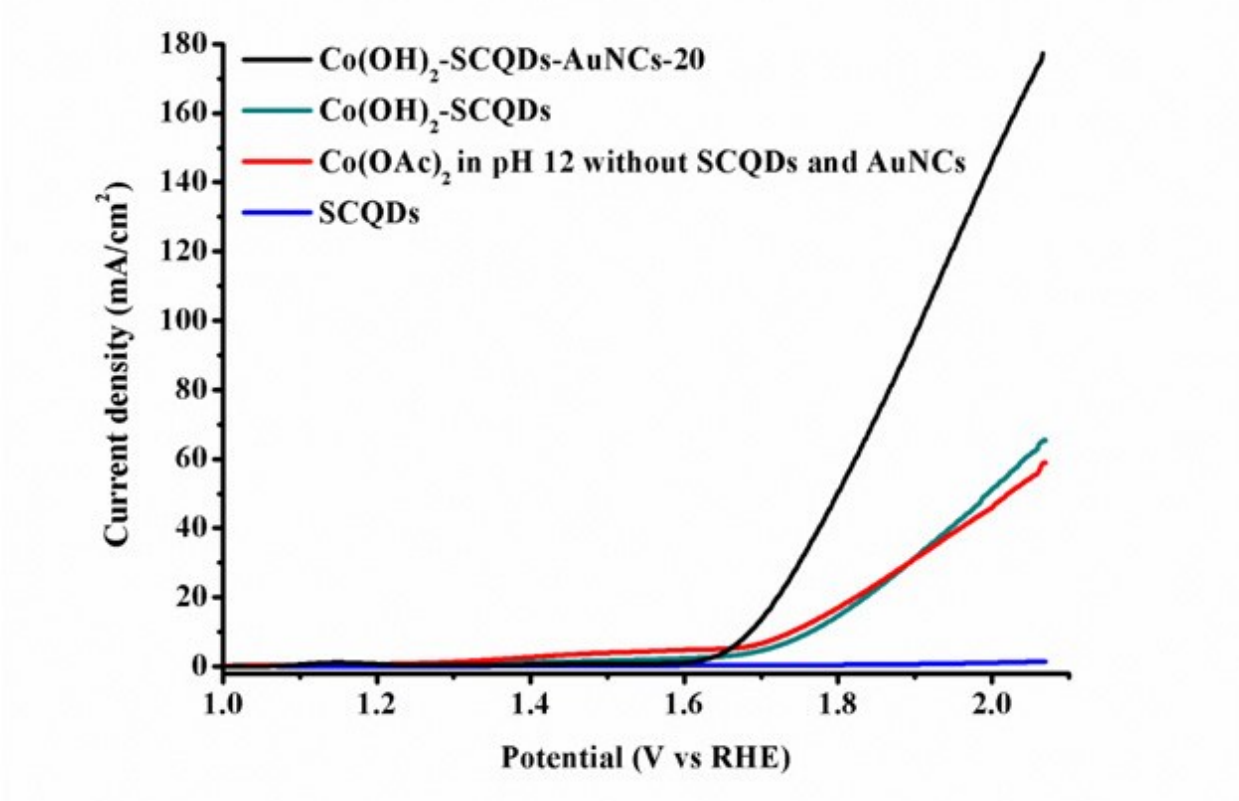

Figure S17. OER LSV curves for Amorphous $Co(OH)_2$ encapsulated by Au-SCQDs-20, un-doped pure $Co(OH)_2$ and Au-SCQDs alone.

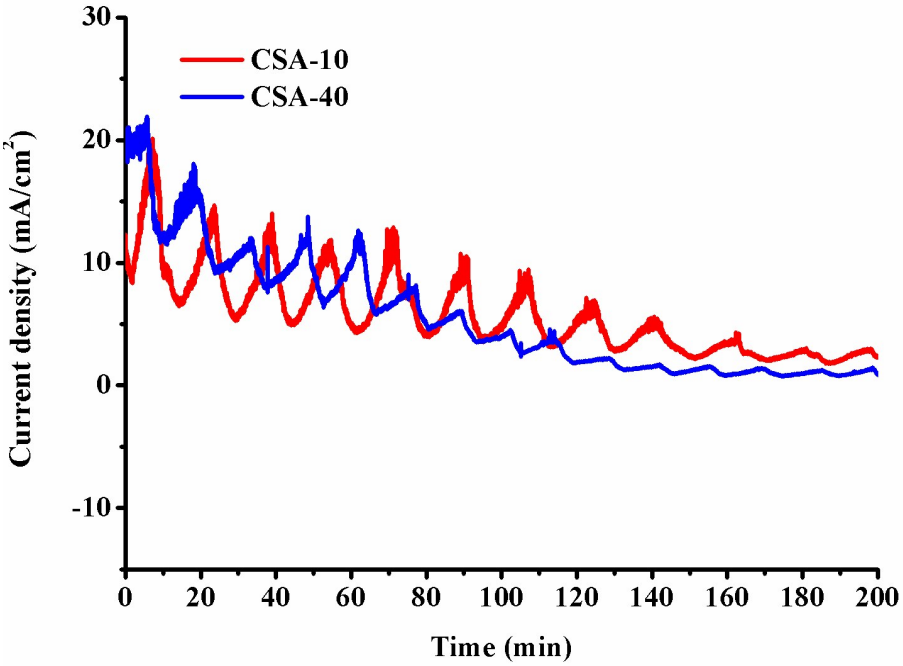

Figure S18. Chronoamperometry of $Co(OH)_2$-Au-SCQDs-10 and 40.

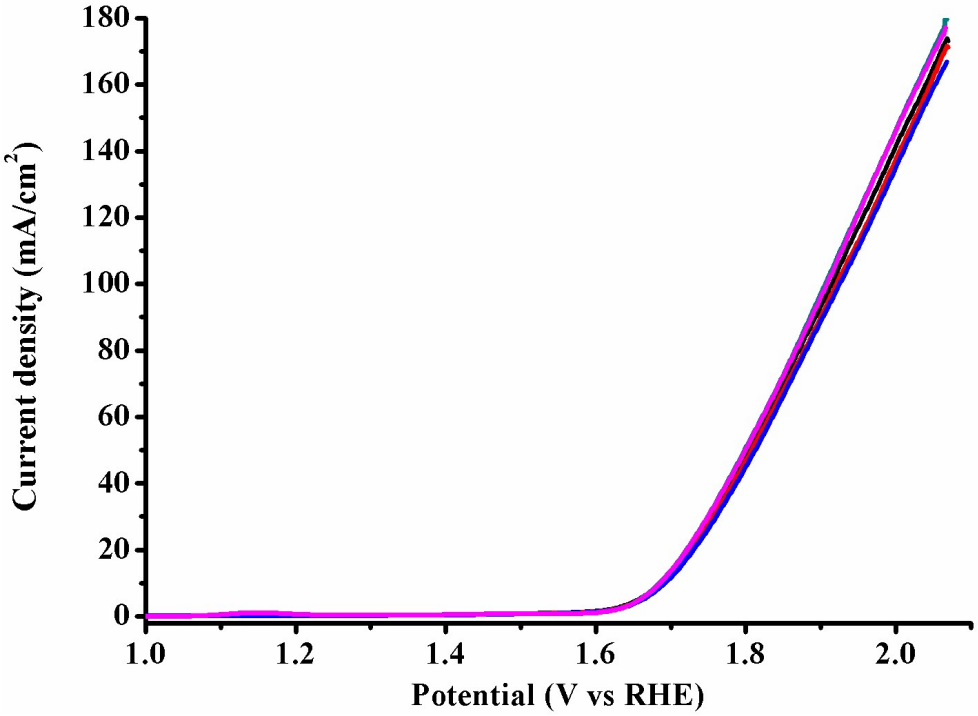

Fig. S19. LSV curve for OER studies of CSA-20 prepared from five different batches.

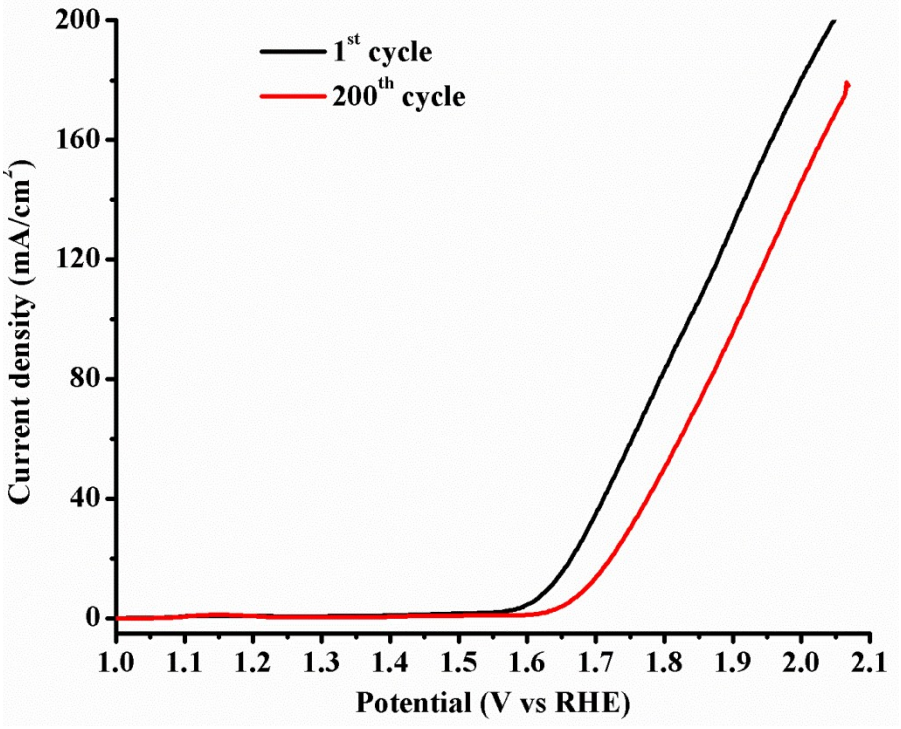

Figure S20. OER LSV curves for 1st & 200th cycle of $Co(OH)_2$-Au-SCQDs-20.

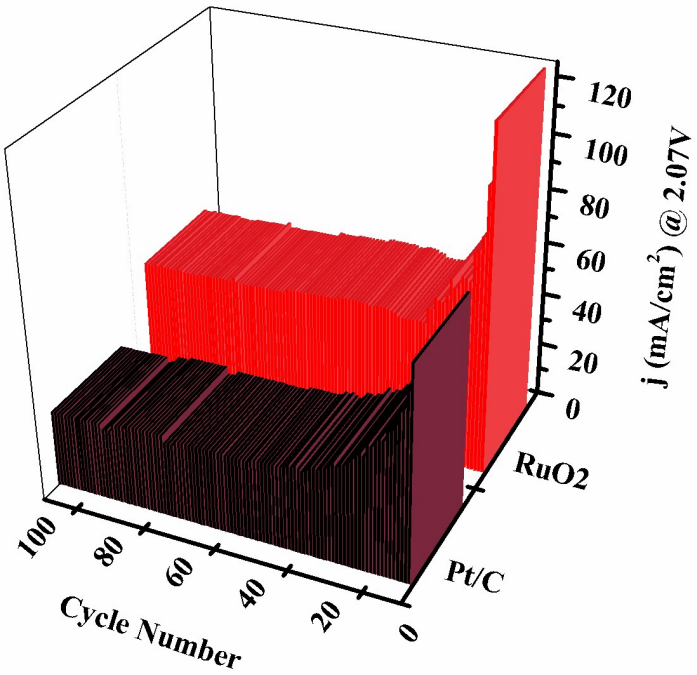

Fig. S21. Stability studies for commercial standard RuO_2 and Pt/C from cyclic voltammetry.

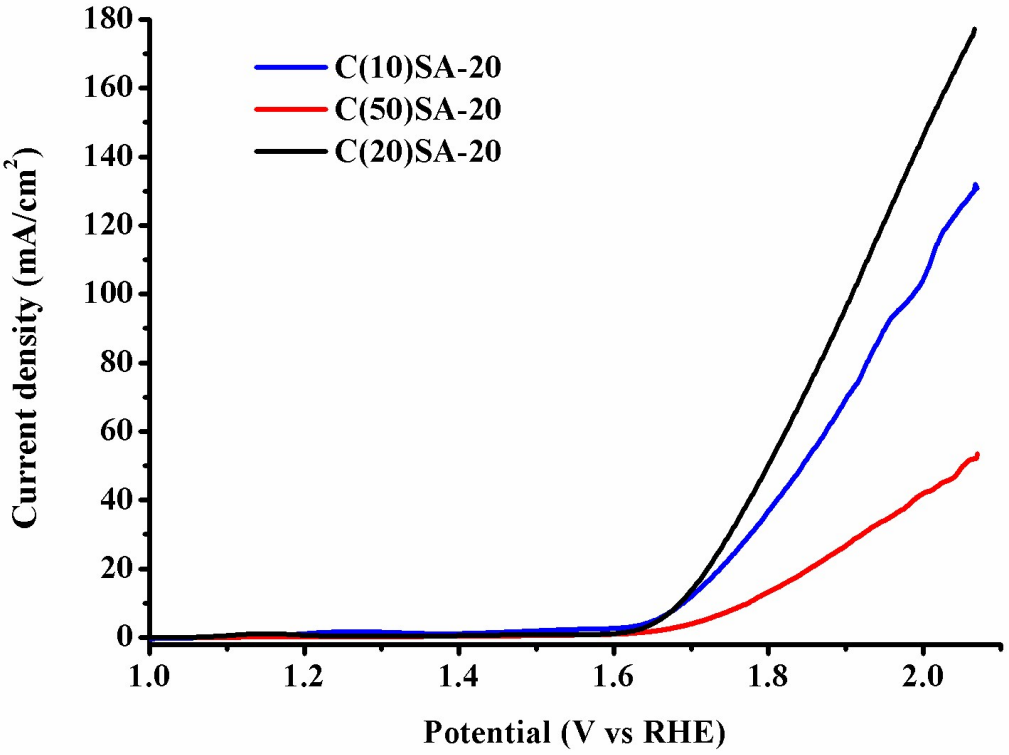

Figure S22. OER LSV curves for Au-SCQDs-20 with different concentration of $Co(OH)_2$-10, 20 & 50.

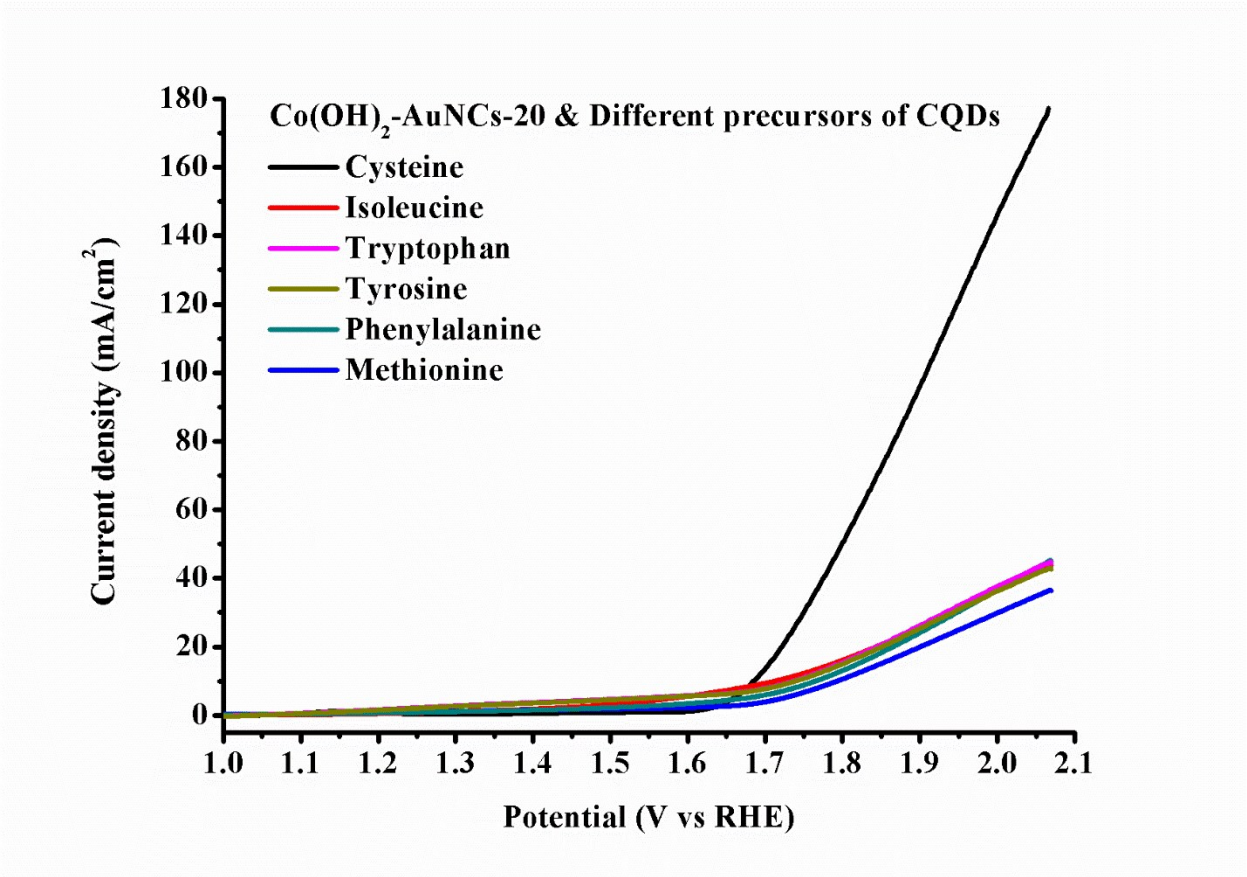

Figure S23. OER LSV curves for $Co(OH)_2$-different precursors of CQDs-AuNCs-20.